

Experimental Investigation of Active Disturbance Rejection Control for Vehicle Suspension Design

Panshuo Li James Lam Kie Chung Cheung
The University of Hong Kong
Department of Mechanical Engineering
Pokfulam Road, Hong Kong
panshuoli812@gmail.com james.lam@hku.hk k.c.cheung@hku.hk

Abstract: This paper investigates the vibration attenuation problem of a vehicle suspension test rig, aiming at stabilizing its attitude. In the presence of nonlinear and unknown system dynamics, an accurate mathematical model of the test rig is not available. Active disturbance rejection control is employed to design a controller. An extended state observer is established to estimate the total disturbance which will be compensated in the controller design. The method will be very useful in industrial applications of active vehicle suspension because of its good robustness and easy implementation. Experimental results under different road profiles are used to validate the merits of the proposed control method.

Key-Words: Active control, disturbance rejection, nonlinear dynamics, vehicle suspension

1 Introduction

Vehicle suspension is used to isolate the vibration induced by road irregularities so as to provide good ride quality for the passenger. Generally speaking, vehicle suspension can be classified into three types, that is, passive, semi-active and active ones. Although the cost of passive suspension is low, its limited performance can hardly meet the complicated design requirements demanded under various road conditions. Semi-active suspension may better tackle such an issue to a certain extent [1, 2], but it does not have good performance as the active one. Active suspension is attracting more and more attention these days because of its excellent performance under different road profiles and high potential to meet tight performance specifications.

Many favorable results have been reported on active vehicle suspension with different kinds of control methods, such as optimal control [3], linear quadratic regulator-based control [4], H_∞ control [5]. In most previous works, in order to conveniently develop the control methods, highly simplified suspension models have been used in designing the controller. It is often assumed that the system is linear and an accu-

rate model is available in advance. Based on these highly simplified mathematical models, good simulation results may be obtained, that is, great ride quality can be achieved, road holding is firmly guaranteed and enough rattle space is ensured theoretically. However, industrial applications of those control methods are far from satisfactory because nonlinear dynamics, uncertainties, actuator time-delay in practice have been ignored. To overcome this difficulty, some improved control methods have thus appeared. Load-dependent and velocity-dependent controllers are presented in [6] and [7] to solve the problems of vehicle body load uncertainty, and vehicle velocity uncertainty with preview strategy, respectively. Many other methods to handle system uncertainties can be found in [8, 9], but the design approaches may be highly conservative. Sliding mode control [10], linearization feedback control [11], parameter varying control [12], backstepping control [13], adaptive control [14] have been adopted to tackle the nonlinear issues in active vehicle suspension system. However, all of these methods have their limitations, such as the chatting phenomenon in the sliding mode control will deteriorate the performance, and only weak nonlinearity is allowed in the operation range of the adaptive control.

In industrial applications, fuzzy control is a popular method in which the model-free property facilitates the controller design. Its applications in active vehicle suspension can be found in [15, 16]. However, fuzzy control requires knowledge and experiences to design the fuzzy rules and membership functions, which may be time-consuming, especially for a complicated system.

Except for some industrial laboratory applications of active vehicle suspensions, for instance, the Bose active suspension, Active Body Control system from Mercedes-Benz model cars, experimental results are not broadly reported in the academic research area. Experimental investigation of multi-objective control with look ahead preview is provided in [17], the experimental results show the effectiveness of the proposed method for a specific test rig. Sliding mode controller combining with an inertial delay observer is proposed to design an active vehicle suspension in [18], both numerical simulation and experimental results under different road conditions have validated its merits.

In this paper, an experimental investigation is carried out for a quarter-car suspension test rig. Active disturbance rejection control (ADRC), as a kind of model-free control scheme, is adopted to design the controller. Within this scheme, the external disturbance and internal unknown dynamics are treated as the total disturbance, which is estimated through an extended state observer and compensated within the controller formulation. ADRC is very suitable for industrial applications, since all the uncertainties, nonlinearities, time-delay and other unknown dynamics can be treated as the total disturbance and it is easy to implement. The experimental results show that the ADRC can achieve good performance under different road profiles. The rest of this paper is organized as follows. The system is described and problem is formulated in Section 2. Section 3 presents the controller synthesis with ADRC. Experimental results are reported in Section 4. Conclusions are provided in Section 5.

2 Model and Problem Formulation

Considering the vertical dynamics of vehicle body and the symmetric structure of a vehicle, a quarter-car model is commonly considered in suspension designs. The quarter-car suspension test rig considered

in this study is shown in Figure 1. Three sliding steel plates can move along the steel shafts with bearings. The blue plate with the mass on it represents the vehicle body (sprung mass), the red plate represents the mass of wheel and its assembly (unsprung mass). The suspension system, placed between the blue and red plates, consists of two symmetric springs and a DC motor in parallel. The tyre is simulated with the springs between red plate and silver plate. Notice that the suspension and tyre damping is inherent in the structure, and the motor only works in the active suspension case. The road profile is imitated by the silver plate moving vertically, which is excited by a DC motor at the bottom.

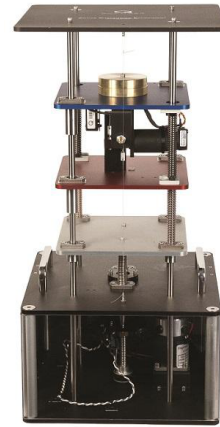


Figure 1: Quarter-car suspension test rig

The schematic structure of the test rig is illustrated in Figure 2, in which m_s stands for the sprung mass, and m_u stands for the unsprung mass. The displacements of sprung mass and unsprung mass are denoted with z_s , z_u , and the road irregularity is represented by z_r . The spring force and damping force of suspension and tyre are represented by F_{ss} , F_{sc} and F_{ts} , F_{tc} , respectively. In the active suspension, u represents the controller force which is generated by the DC motor in this case. Then, the system dynamics can be given as

$$\begin{aligned} m_s \ddot{z}_s &= -F_s - u, \\ m_u \ddot{z}_u &= F_s + F_t + u, \end{aligned} \quad (1)$$

where F_s , F_t are suspension force and tyre force, respectively, with $F_s = F_{ss} + F_{sc}$, $F_t = F_{ts} + F_{tc}$. If the suspension components are linear, and let k_s , c_s

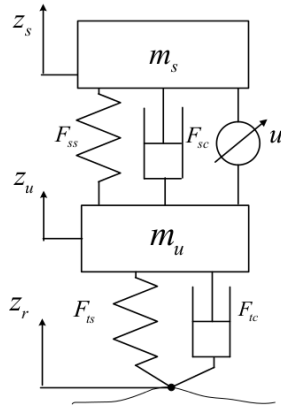


Figure 2: Schematic structure of test rig

denote the suspension stiffness and damping coefficient, respectively, and k_t , c_t represent the tyre stiffness and damping coefficient, respectively, then F_{ss} , F_{sc} , F_{ts} , F_{tc} can be given as

$$\begin{aligned} F_{ss} &= k_s(z_s - z_u), \\ F_{ds} &= c_s(\dot{z}_s - \dot{z}_u), \\ F_{ts} &= k_t(z_u - z_r), \\ F_{td} &= c_t(\dot{z}_u - \dot{z}_r). \end{aligned} \quad (2)$$

However, nonlinearities are always present in practice, which can be classified into the following forms:

- Nonlinear suspension spring: pneumatic spring, force can be modeled as the linear part combining with a quadratic term of the relative displacement, that is,

$$F_{ss} = k_s(z_s - z_u) + k_{ns}(z_s - z_u)^3$$

where k_{ns} is the coefficient of the nonlinear term.

- Nonlinear suspension damper: damping coefficients of the extension and compression travel are different, or the damper displays nonlinear velocity-force relations, as Figure 3 shows.

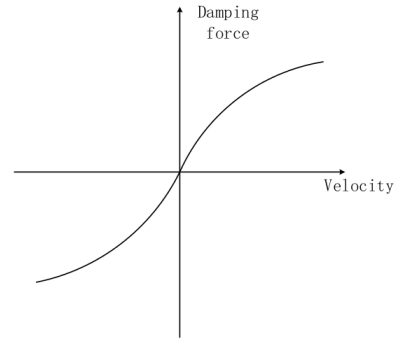


Figure 3: Illustration of a nonlinear damper

- Friction: bearing friction or the friction between sliding plate and shaft.
- Nonlinear tyre dynamics: nonlinear characteristics derived from the rubber material.

Other sources of nonlinearity may due to the misalignment of damper/spring pair with the body and wheel masses [17]. For our test rig, the system nonlinearity is present but cannot be accurately modeled. The nominal coefficients of the system are listed in Table 1. It is worth mentioning that although the nominal coefficients are provided here, they are not needed for controller development.

Table 1: Nominal coefficients of the model parameters

| | | | |
|-------|---------|-------|----------|
| m_s | 2.45 kg | c_s | 7.5 Ns/m |
| m_u | 1 kg | k_t | 1250 N/m |
| k_s | 900 N/s | c_t | 5 Ns/m |

Vehicle suspension, as an important vehicle component, plays a vital role in vibration isolation. For an active suspension, the controller needs to provide force to stabilize the vehicle body attitude, that is, to attenuate the vertical displacement of the sprung mass in quarter-car case. Apart from providing good ride quality, the suspension needs to guarantee ride safety, which means the tyres need to firmly contact with the road. Since the tyre behaves as an elastic element, the specification is always measured by the tyre deflection. Moreover, a suspension needs to avoid mechanical damage, so it should ensure an enough rattle space to protect the vehicle body from bottoming.

In summary, the design objective of an active vehicle suspension is as follows:

Objective: For a vehicle suspension test rig, design a controller to attenuate the vertical vibration of the sprung mass of the closed-loop system, and to ensure enough rattle space and the tyre deflection is in the acceptable range.

3 Active Disturbance Rejection Controller Synthesis

Many control methods have been proposed for active vehicle suspension, and most of them are based on an accurate suspension model. The performance of these methods are often far from satisfactory when tested by experiments or applied in real situations. In this section, we design an active disturbance rejection controller for a test rig with unmodelled dynamics, to attenuate the vertical displacement of the sprung mass for good ride comfort.

The disturbance rejection idea was established decades ago, and Han rekindled this idea in 1990s and formally introduced the concept of ADRC [19]. In recent years, ADRC is employed in many areas of engineering practice [20–22], but seldom one finds an integrated application of ADRC in vehicle suspension. In the following, we will provide the process of ADRC controller synthesis of the vehicle suspension. The dynamic equation of the sprung mass can be given as

$$\begin{aligned} \ddot{z}_s &= F(t, z_s, \dot{z}_s, z_u, \dot{z}_u) - bu, \\ y &= z_s, \end{aligned} \quad (3)$$

where $F(t, z_s, \dot{z}_s, z_u, \dot{z}_u) = -F_s + F_\Delta$ represents the total disturbance with F_Δ denotes the unknown disturbance, and $b = \frac{1}{m_s}$. The closed-loop system with ADRC is shown in Figure 4. It can be seen that the ADRC consists of three components, namely, a track differentiator (transient profile generator), an extended state observer, and a nonlinear control feedback. v_0 is the control objective signal, v_1 is the tracking signal of v_0 , and v_2 is the derivative signal of v_1 ; p_1 , p_2 are estimates of the system measurement output y and its derivative signal, and p_3 is the estimate of the total disturbance $F(t, z_s, \dot{z}_s, z_u, \dot{z}_u)$; e_1, e_2 are the error signals, and u_0 is the output of the nonlinear con-

troller. Note that the total disturbance F is assumed to be differentiable with respect to time.

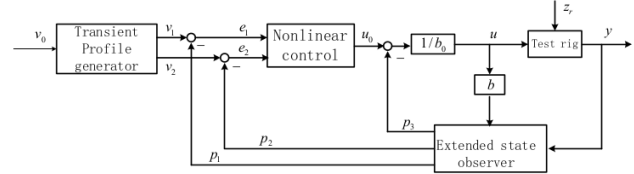


Figure 4: Structure of ADRC Scheme

First, a track differentiator is established to obtain the tracking signal of the control objective signal v_0 and its derivative. Constructing a track differentiator in the following form

$$\begin{cases} \dot{v}_1 = v_2, \\ \dot{v}_2 = -r \operatorname{sgn} \left(v_1 - v_0(t) + \frac{v_2 |v_2|}{2r} \right), \end{cases} \quad (4)$$

where $r > 0$ is a constant which can be selected to speed up or slow down the transient profile.

The main objective of ADRC is to estimate the total disturbance and reject its effects. For the vehicle suspension system (3), choose state vector $x = [x_1, x_2]^T$, where $x_1 = z_s$, $x_2 = \dot{z}_s$. Treating the total disturbance as an additional state variable, that is, $x_3 = F(t, z_s, \dot{z}_s, z_u, \dot{z}_u)$, and let $\dot{F}(t, z_s, \dot{z}_s, z_u, \dot{z}_u) = G(t)$, with $G(t)$ unknown. Then, system (3) can be described as

$$\begin{cases} \dot{x}_1 = x_2, \\ \dot{x}_2 = x_3 - bu, \\ \dot{x}_3 = G(t), \\ y = x_1, \end{cases} \quad (5)$$

Establish an extended state observer in the form of

$$\begin{cases} e = p_1 - y, \\ f_{e0.5} = \operatorname{fal}(e, 0.5, \delta), \quad f_{e0.25} = \operatorname{fal}(e, 0.25, \delta) \\ \dot{p}_1 = p_2 - \beta_{01}e \\ \dot{p}_2 = p_3 + bu - \beta_{02}f_{e0.5}, \\ \dot{p}_3 = -\beta_{03}f_{e0.25}, \end{cases} \quad (6)$$

where

$$\operatorname{fal}(e, \alpha, \delta) = \begin{cases} \frac{e}{\delta^{1-\alpha}}, & |e| \leq \delta, \\ |e|^\alpha \operatorname{sgn}(e), & |e| \geq \delta, \end{cases}$$

and $\beta_{01}, \beta_{02}, \beta_{03}, \delta$ are positive constants. It can be seen that the established extended state observer only needs the system output y and the control input u , the output of the observer includes the estimate of the system total disturbance $F(t, z_s, \dot{z}_s, z_u, \dot{z}_u)$ and the original system state.

With the total disturbance information obtained from the extended state observer, the control input u can be constructed based on the disturbance rejection concept, that is,

$$u = \frac{u_0 - p_3}{b_0},$$

with $b_0 \approx b$. The control u_0 can be designed as a nonlinear feedback given by

$$u_0 = \beta_1 \text{fal}(e_1, \alpha_1, \delta) + \beta_2 \text{fal}(e_2, \alpha_2, \delta). \quad (7)$$

where $e_1 = v_1 - p_1$, $e_2 = v_2 - p_2$. Notice that u_0 can be obtained from a simple PD formulation, but the nonlinear feedback (7) shows better performance in practice [3].

4 Experimental Results

In this section, the proposed control method is carried out on the test rig. The control law is implemented with Matlab/Simulink and the excitation signal of the DC motor is generated using Simulink for the road profile. The suspension deflection and tyre deflection signals are captured by two 10-bit optical encoders, then the measurement output y can be computed as a combination of the road signal and the encoder signals. The full experimental setup is shown in Figure 5. It can be seen that apart from the suspension test rig (A in figure), the hardware setup consists of a data acquisition card (B in figure), a power amplifier (C in figure) and a computer (D in figure).

The controller parameters are chosen according to [19], which are given as $\beta_{01} = 75, \beta_{02} = 1875, \beta_{03} = 15625, \delta = 0.005, \beta_1 = 25, \beta_2 = 10$. The control objective v_0 is chosen as $v_0 = c(z_s - z_u)$ to ensure enough rattle space with $c = 0.5$.

Experiments are carried out under different road profiles. It should be mentioned that the disturbance magnitude in experiments are proportional to the disturbance magnitude in practice due to that the test rig is a scaled model. First, to clearly illustrate the performance, a sinusoidal signal is adopted as the disturbance input, given by $z_0 = 0.002 \sin(6\pi t)$. The

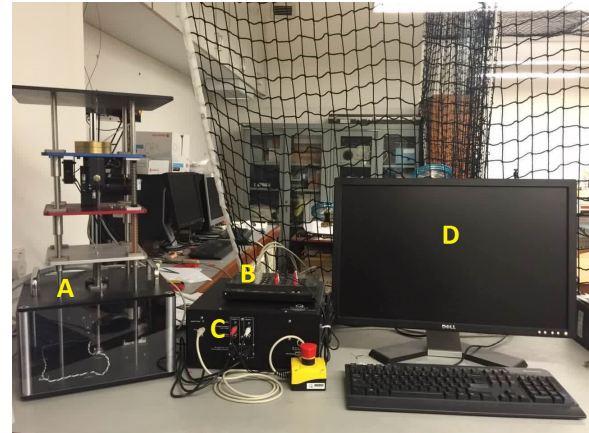


Figure 5: Experimental setup of the active control

system responses of the open and closed-loop system are compared in Figure 6, and the suspension deflection and tyre deflection are shown in Figure 7. It can be observed that vertical motion of the sprung mass is significantly attenuated, and the suspension and tyre deflections are within acceptable ranges.

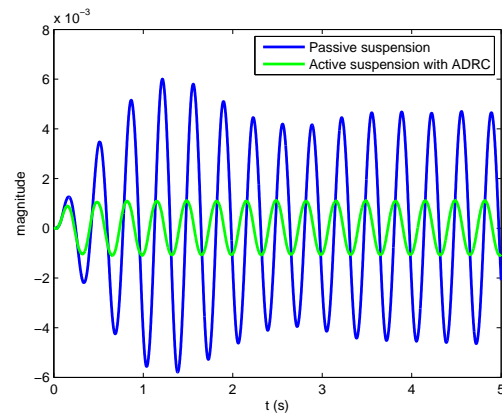


Figure 6: System responses comparison under sinusoidal road profile

Then a stochastic disturbance is considered. A practical stochastic road profile description may be given by

$$\dot{w} = -2\pi q_0 v w + 2\pi \sqrt{G_0} v w_0,$$

where q_0 is the reference spatial frequency and v is the vehicle forward velocity, G_0 is the road roughness coefficient, w_0 is white noise with unit variance. Choose

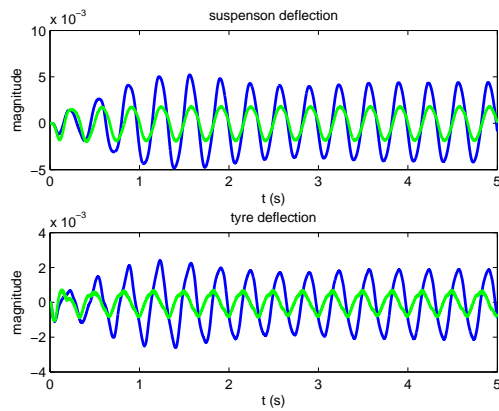


Figure 7: Suspension and tyre deflections under sinusoidal road profile

$G_0 = 256 \times 10^{-6}$, $q_0 = 0.01$, $v = 20$. The excitation for this test rig can be given as $z_r = dw$ with d is a scaling coefficient, which is chosen as 0.1.

The vertical displacements of the sprung mass of open and closed-loop system under stochastic disturbance input are shown in Figure 8, the suspension deflection and tyre deflection are shown in Figure 9. It can be observed that the active suspension provides a significant reduction of vibration, and the suspension deflection and tyre deflection have little difference from the passive case.

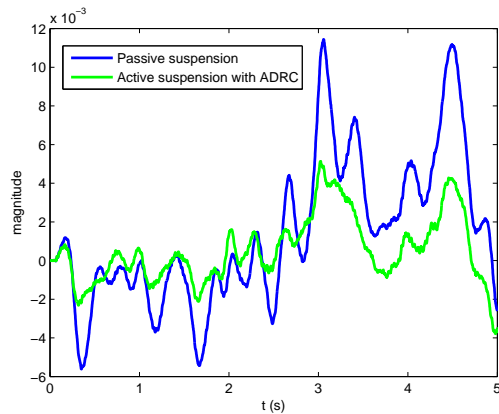


Figure 8: System responses comparison under stochastic road profile

Finally, consider another common road profile,

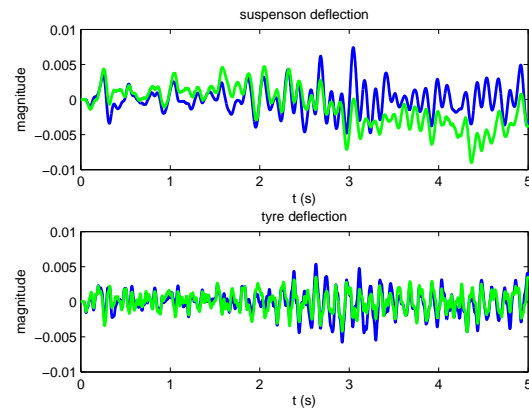


Figure 9: Suspension and tyre deflections under stochastic road profile

that is, a bump road profile given by

$$z_r = \begin{cases} \frac{h(1-\cos(8\pi v))}{2}, & 1 < t < 1.25, \\ 0, & \text{otherwise.} \end{cases}$$

where h is the height of the bump and set as 0.02 m. The system response comparisons of open and closed-loop systems are shown in Figure 10, and the corresponding suspension deflection and tyre deflection are given in Figure 11. It can be seen that under this road profile, the vehicle attitude of the sprung mass is quickly stabilized by the proposed controller, and the suspension deflection and tyre deflection are within their acceptable ranges as well.

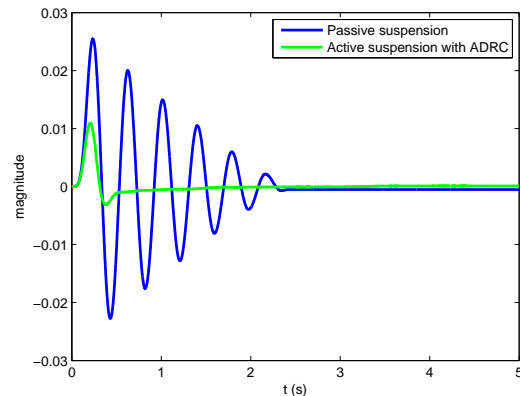


Figure 10: System responses comparison under bump road profile

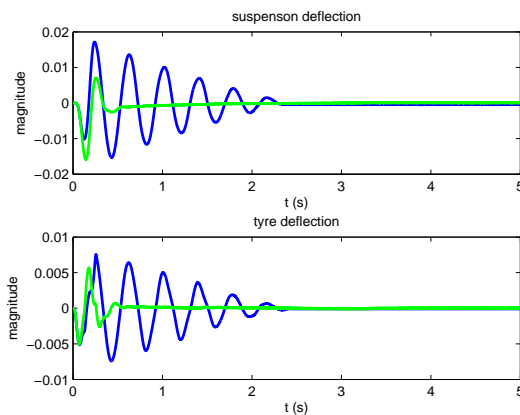


Figure 11: Suspension and tyre deflections under bump road profile

5 Conclusion

In this paper, active disturbance rejection control is employed to stabilize the vehicle body attitude of a suspension test rig. The total disturbance consisting of external excitation and internal nonlinear unknown dynamics can be estimated with an extended state observer, and compensated by the controller. This method is very effective for active suspension design in practice because of its good robustness, high vibration attenuation performance and easy implementation. The experimental results under different road profiles have illustrated that the proposed method can successfully attenuate the sprung mass vibration and keep the suspension deflection and tyre deflection within their acceptable ranges.

References:

- [1] H. Chen, C. Long, C. Yuan, and H. Jiang. Non-linear modelling and control of semi-active suspensions with variable damping. *Vehicle System Dynamics*, 51(10):1568–1587, 2013.
- [2] P. Li, J. Lam, and K. C. Cheung. Control of vehicle suspension using an adaptive inerter. *Proceedings of the Institution of Mechanical Engineers Part D- Journal of Automotive Engineering*, 10pp, 2015.
- [3] S. Y. Han, G. Y. Tang, and X. X. Yang. Optimal vibration control for vehicle active suspension discrete-time systems with actuator time delay. *International Journal of Control*, 34(5):1641–1645, 2013.
- [4] H. D. Taghirad. Automobile passenger comfort assured through LQG/LQR active suspension. *Journal of Vibration and Control*, 4(5):603–618, 1998.
- [5] P. Li, J. Lam, and K. C. Cheung. Multi-objective control for active suspension with wheelbase preview. *Journal of Sound and Vibration*, 333(21):5269–5282, 2014.
- [6] H. Gao, J. Lam, and C. Wang. Multi-objective control of vehicle active suspension systems via a load-dependent controllers. *Journal of Sound and Vibration*, 290(3-5):654–675, 2006.
- [7] P. Li, J. Lam, and K. C. Cheung. Velocity-dependent multi-objective control of vehicle suspension with preview measurements. *Mechatronics*, 2014.
- [8] H. Du, N. Zhang, and J. Lam. Parameter-dependent input-delayed control of uncertain vehicle suspensions. *Journal of Sound and Vibration*, 317(3-5):537–556, 2008.
- [9] H. Du, N. Zhang, and F. Naghdy. Robust control of vehicle electrorheological suspension subject to measurement noises. *Vehicle System Dynamics*, 49(1-2):257–275, 2011.
- [10] A. J. Koshkouei and K. J. Burnham. Sliding mode controllers for active suspensions. In *Proceeding of the 17th IFAC World Congress*, pages pp 1–6, Seoul, Korea, 2008.
- [11] H. Pan, W. Sun, H. Gao, T. Hayat, and F. Alsaadi. Nonlinear tracking control based on extended state observer for vehicle active suspensions with performance constraints. *Mechatronics*, 2014.
- [12] I. Fialho and G.J. Balas. Design of nonlinear controllers for active vehicle suspensions using parameter-varying control synthesis. *Vehicle System Dynamics*, 33(5):351–370, 2000.
- [13] W. Sun, H. Gao, and O. Kaynak. Adaptive backstepping control for active suspension system with hard constraints. *IEEE-ASME Transactions on Mechatronics*, 18(3):1072–1079, 2013.
- [14] W. Sun, H. Gao, and B. Yao. Adaptive robust vibration control of full-car active suspensions with electrohydraulic actuators. *IEEE Transactions on Control Systems Technology*, 21(6):2417–2422, 2013.

- [15] H. Du and N. Zhang. Fuzzy control for non-linear uncertain electrohydraulic active suspension with input constraint. *IEEE Transactions on Fuzzy Systems*, 17(2):343–356, 2009.
- [16] H. Du and N. Zhang. Takagi-Sugeno fuzzy control scheme for electrohydraulic active suspensions. *Control and Cybernetics*, 39(4):1095–1115, 2010.
- [17] A. Akbari, G. Koch, E. Pellegrini, and B. Lohmann. Multi-objective preview control of active vehicle suspensions: Experimental results. *Advanced Computer Control*, 3:497–502, 2010.
- [18] S. Gupta, D. Ginoya, P. D. Shendge, and S. B. Phadke. An inertial delay observer-based sliding mode control for active suspension systems. *Proc IMechE Part D: Journal of Automobile Engineering*, 1(19):19pp, 2015.
- [19] J. Han. From PID to active disturbance rejection control. *IEEE Transactions on Industrial Electronics*, 56(3):900–906, 2009.
- [20] G. Feng, Y. Liu, and L. Huang. A new robust algorithm to improve the dynamic performance on the speed control of induction motor drive. *IEEE Transactions on Power Electronics*, 6:1614–1627, 2004.
- [21] D. Wu, K. Chen, and X. Wang. Tracking control and active disturbance rejection with application to noncircular machining. *International Journal of Machine Tools and Manufacture*, 47(15):2207–2217, 2007.
- [22] Y. Huang, K. Xu, J. Han, and J. Lam. Flight control design using extended state observer and non-smooth feedback. In *Proceeding of 40th Conference on Decision and Control*, pages 223–228, Orlando, USA, 2001.